W^+W^- and Z^0Z^0 pair production in e^+e^-, pp, and $\bar{p}p$ colliding beams

R. W. Brown

Physics Department, Case Western Reserve University, Cleveland, Ohio 44106

K. O. Mikaelian*

Fermi National Accelerator Laboratory, Batavia, Illinois 60510
and Department of Physics and Astronomy, Northwestern University, Evanston, Illinois 60201

We discuss the production of pairs of weak bosons in those processes where electrons or quarks annihilate. Besides comparing and extending previous calculations for $e^+e^- \rightarrow W^+W^-$, we consider $e^+e^- \rightarrow Z^0Z^0$, pp and $p\bar{p} \rightarrow W^+W^-X$ or Z^0Z^0X. It is emphasized that (1) the rate of production of Z^0 pairs is comparable to that of W pairs and that (2) W-pair production with colliding proton beams may be the best way to see high-energy cancellations in cross sections, the hallmark of renormalizability in gauge theories.

I. INTRODUCTION

Whether or not we can describe weak interactions with a renormalizable local field theory is at the heart of the ongoing search for the intermediate vector bosons. Theoretically, the gauge principle used in the archetypal Weinberg-Salam model[1] is so attractive (renormalizability, neutral currents, etc.) that we have come to believe *a fortiori* in the existence of at least a triplet $W^\pm, Z^0$ of these particles, particularly as "gauge" bosons. This belief carries along with it the predicted mass range of 30–100 GeV/c^2 as a good bet.

Experimentally, the mass range explains why we have not seen evidence for the weak bosons even as propagator effects.[2] No present machine produces a large enough c.m. energy. The experiments on atomic parity violation notwithstanding, all of the weak-interaction phenomena are nicely embraced by such a theory.[3] (The resolution of the dilemma in atomic physics may reside in a more refined theoretical analysis or perhaps in the fact that more neutral bosons exist.) It is generally felt, however, that the true test will come with the next generation of high-energy accelerators where the threshold for actual production can be reached.

The production of these putative particles is in fact a primary goal of the proposed machines. For example, ISABELLE[4] may attain several hundred GeV in c.m. energy with its colliding proton beams. Electron-proton and even electron-positron colliding beams of comparable energies are in the planning stage as well.[5]

These plans require, of course, some idea of what to expect in the way of rates and signature for such production events. In the past, we have seen many theoretical estimates of specific production cross sections for a variety of "beams" and "targets." With the coming of ISABELLE and other similar facilities,[6] recent efforts have concentrated on proton-proton, and antiproton-proton collisions.[7] The conclusions are generally promising although problems may arise from uncertainties in the decay branching ratios, in "new physics" backgrounds, and in the extrapolation of the Drell-Yan approximation into new energy regimes.

In this paper, we respond to the possibility that in this next generation of accelerators the threshold for pair production may be passed as well. The goal is to present estimates of the rates and to point out the dependence of the result on boson trilinear couplings and the charm quark. Gauge-theory cancellations at high energy may therefore be observed, possibly for the first time.

We have another reason for our interest in pairs. In electron-positron collisions, single $W^\pm$ production is higher order than the W^+W^- pair creation. There is roughly a three-orders-of-magnitude difference in the cross sections in the mass-energy regime of interest. Although the reaction $e^+e^- \rightarrow W^+W^-$ has been studied in some detail recently, we notice that $e^+e^- \rightarrow Z^0Z^0$ is almost as probable for comparable masses. This has not been discussed previously to our knowledge, but if $e^+e^- \rightarrow W^+W^-$ ever becomes accessible, than $e^+e^- \rightarrow Z^0Z^0$ will also. One compares these reactions rather naturally as a preliminary to the proton-proton study inasmuch as that study requires the same Dirac point-particle annihilation. Therefore this paper includes some conclusions about pair production via e^+e^- collision as we move toward the colliding-proton-beam case.

The next two sections carry a discussion of general calculational procedures, assumptions, and approximations used in our analysis of these pair production channels. In Sec. IV, we give differential- as well as total-cross-section results for the electron-positron colliding beams. There is some overlap here with previous papers but for

completeness we do include some W^+W^- curves. Here and later we give examples of simple "fits" to the total cross section as a function of energy and mass; the intent is to provide experimentalists with mnemonics for extrapolating to other regions not explicitly given.

We focus on W^+W^- and Z^0Z^0 pair production rates for pp and $p\bar{p}$ collisions in Sec. V. An attempt is made to compare the size of the signal with that for single $W^\pm$, Z^0 production. Finally, we discuss the directions that our results indicate might be best for future plans. This and sundry remarks comprise Sec. VI.

II. CALCULATIONAL PRELIMINARIES

The amplitudes for Dirac point-particle annihilation into weak-boson pairs can be calculated in lowest order once the couplings have been determined. In this section, we lay out the familiar theoretical underpinnings to that end and, in the next section, the specific amplitudes are constructed.

The couplings are given to us, for example, in the SU(2)⊗U(1) Weinberg-Salam gauge model generalized to include quarks.[8] Since we are merely after order-of-magnitude accuracy, the specific model is not of great consequence. On the other hand, it will not be hard for the reader to adapt our results to other theories—often a simple multiplicative factor will do—however transmogrified. Indeed, the variety and couplings of Z^0's are currently controversial.

The relevant fermion (electron, electron neutrino, and four quarks) part of the interaction Hamiltonian is[1,8,9]

$$\mathcal{H}_{\text{fermion}} = \sum_{i=e,u,d,s,c} [eQ_i\bar{\psi}_i\gamma^\mu\psi_i A_\mu$$
$$+\bar{\psi}_i\gamma^\mu(g_V^i - g_A^i\gamma_5)\psi_i Z_\mu]$$
$$+ \sum_{\substack{i=e,d,s \\ j=\nu_e,u,c}} G_{V-A}^{ij}[\bar{\psi}_i\gamma^\mu(1-\gamma_5)\psi_j W_\mu + \text{H.c.}], \tag{2.1}$$

where the charges ("electromagnetic neutral-current couplings") are

$$Q_e = -1, \quad Q_u = Q_c = \tfrac{2}{3}, \quad Q_d = Q_s = -\tfrac{1}{3}, \tag{2.2}$$

and the weak charged-current couplings can be summarized by

$$G_{V-A}^{ij} = \frac{M_W\sqrt{G_F}}{2^{1/4}}[\delta_{ie}\delta_{j\nu_e} + (\cos\theta_C\delta_{id} + \sin\theta_C\delta_{is})\delta_{ju}$$
$$+ (\cos\theta_C\delta_{is} - \sin\theta_C\delta_{id})\delta_{jc}]. \tag{2.3}$$

Also, the weak neutral couplings are given by

$$\begin{pmatrix} g_V^i \\ g_A^i \end{pmatrix} = 2^{1/4}M_Z\sqrt{G_F}\begin{pmatrix} a_i \\ b_i \end{pmatrix} \tag{2.4}$$

with

$$a_e = -\tfrac{1}{2} + 2x, \quad a_u = a_c = \tfrac{1}{2} - \tfrac{4}{3}x, \quad a_d = a_s = -\tfrac{1}{2} + \tfrac{2}{3}x,$$
$$b_e = b_d = b_s = -\tfrac{1}{2}, \quad b_u = b_c = \tfrac{1}{2}. \tag{2.5}$$

High-energy neutrino-physics data point toward a Weinberg angle corresponding to

$$x \equiv \sin^2\theta_W \simeq 0.3 \tag{2.6}$$

or $\theta_W \simeq 33°$. The Cabibbo angle is also an experimental input: $\sin^2\theta_C \simeq 0.06$.

In addition, we need the interaction of the bosons, γ, $W^\pm$, and Z^0 among themselves. Ignoring e^2 terms which do not contribute to our amplitudes in lowest order, there are only trilinear couplings:

$$\mathcal{H}_{\text{boson}} = ie[(A^\nu W^\mu - A^\mu W^\nu)\partial_\mu W_\nu^\dagger$$
$$- (A^\nu W^{\dagger\mu} - A^\mu W^{\dagger\nu})\partial_\mu W_\nu$$
$$+ (\partial^\mu A^\nu - \partial^\nu A^\mu)W_\mu W_\nu^\dagger] + ie\cot\theta_W[A \to Z]. \tag{2.7}$$

In this theory it is seen that there is no "anomalous" electric quadrupole degree of freedom and that the magnetic dipole moment parameter κ has been fixed:

$$\kappa = 1. \tag{2.8}$$

Thus the associated moments

$$\mu_W = \frac{e}{2M_W}(1+\kappa), \quad Q_W = -\frac{e}{M_W^2}\kappa \tag{2.9}$$

are also fixed.

Accepting the value (2.6), the masses are also fixed in the Weinberg-Salam model:

$$M_W = M_Z\cos\theta_W = \frac{1}{\sin\theta_W}\left(\frac{\pi\alpha}{\sqrt{2}G_F}\right)^{1/2} \simeq \frac{38}{\sin\theta_W}\text{ GeV}/c^2 \tag{2.10}$$

or

$$M_W \simeq 69 \text{ GeV}/c^2, \quad M_Z \simeq 82 \text{ GeV}/c^2. \tag{2.11}$$

The constraints in (2.10) permit us to rewrite the outside factors in the couplings (2.3) and (2.4) as

$$e_W \equiv \frac{M_W\sqrt{G_F}}{2^{1/4}} = \frac{e}{2\sqrt{2}\sin\theta_W},$$

$$e_N \equiv 2^{1/4}M_Z\sqrt{G_F} = \frac{e}{\sin2\theta_W}. \tag{2.12}$$

Including the definition

$$e_Z \equiv e\cot\theta_W, \tag{2.13}$$

we list the specific Feynman rules in Fig. 1. This should be helpful for those readers who are interested in other theories. (See the remarks at the beginning of this section).

Although boson masses are fixed, they do effectively cancel in those formulas which can be compared to the known "low-energy" weak-interaction phenomena. It follows that we could relax the mass restriction in some production processes and yet remain consistent with what is known about the couplings. However, cancellations at high (and sometimes not so high) energy for W^+W^- pair production would then not occur. This is precisely the point of renormalizability and the attendant suppression of high-energy growth of cross sections. We therefore can consider the boson masses as free parameters only at the cost of varying (2.6) and/or affecting the cancellations. Since an additional principle which guides us is that the mass is ultimately an experimental question, we would like to show rates as a function of mass. Somewhat inconsistently then, we may free θ_W and consider the mass range

$$M = 50, \ 75, \ 100, \ 125, \ 150 \ \text{GeV}/c^2 \qquad (2.14)$$

in our calculations. If M_W follows this range, we have

$$x \simeq 0.578, \ 0.257, \ 0.144, \ 0.0927, \ 0.0642 \qquad (2.15)$$

Propagators

Vertices

Wave Functions

FIG. 1. The Feynman rules used in the body of calculations presented here. We ignore fermion (f_i) masses at the very high energies needed for boson production.

and

$$M_Z \simeq 77, 87, \ 108, \ 131, \ 155 \ \text{GeV}/c^2 . \qquad (2.16)$$

If M_Z follows the range in (2.14), then θ_W is complex for the lower values and we must abandon some of our constraints. We return to these questions later.

When we get to proton colliding beams where the quark couplings are to be used, we will also need the distributions of the quarks in the nucleon. This is discussed in Sec. V.

III. FERMION ANNIHILATION RATES

We address ourselves now to the basic reactions

$$f_i + \bar{f}_i \to Z^0 + Z^0 \qquad (3.1)$$

and

$$f_i + \bar{f}_i \to W^+ W^- , \qquad (3.2)$$

where Dirac point fermions (electrons or quarks) annihilate to produce boson pairs. We can consequently discuss colliding-electron-beam experiments and also colliding-proton-beam experiments in the Drell-Yan approximation. The general amplitude is pictured in Fig. 2 together with the momentum assignments. The reduced amplitude $T_{\mu\nu}$ is also defined there.

For reaction (3.1), the lowest-order graphs are shown in Fig. 3 where only the weak neutral-current couplings in Eq. (2.1) contribute. We obtain

$$T^Z_{\mu\nu} = -i(g_V^{i2} + g_A^{i2} + 2g_V^i g_A^i \gamma_5)\left(\gamma_\mu \frac{1}{\not{l}_1}\gamma_\nu + \gamma_\nu \frac{1}{\not{l}_2}\gamma_\mu\right)$$

$$(3.3)$$

with $m_{f_i} = 0$. In terms of the usual variables

$$s = (k_1 + k_2)^2 = (p_1 + p_2)^2 ,$$

$$t = l_1^2 = (k_1 - p_1)^2 = (p_2 - k_2)^2 ,$$

$$u = l_2^2 = (k_1 - p_2)^2 = (p_1 - k_2)^2 , \qquad (3.4)$$

$$s + t + u = 2M_Z^2 ,$$
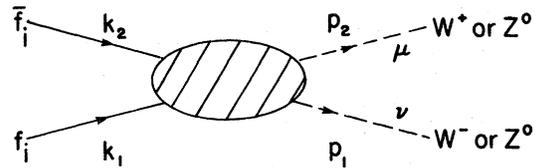
$$= \bar{v}(k_2)T^{\mu\nu}u(k_1)\epsilon_\mu^+(p_2)\epsilon_\nu(p_1)$$
$$\text{or}$$
$$\epsilon_\nu^+(p_1)$$

FIG. 2. The general amplitude for fermion annihilation into weak-boson pairs.

FIG. 3. The lowest-order Feynman diagrams for f_i $+\bar{f}_i \to Z^0 + Z^0$.

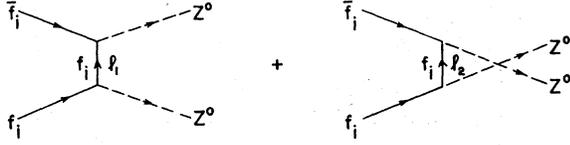FIG. 4. The lowest-order Feynman diagrams for f_i $+\bar{f}_i \to W^+ + W^-$.

the unpolarized differential cross section is

$$\frac{d\sigma^Z}{dt} = \frac{2\pi\alpha^2}{s^2} \frac{g_V^{i4}+g_A^{i4}+6g_V^{i2}g_A^{i2}}{e^4}$$
$$\times \left[\frac{t}{u} + \frac{u}{t} + \frac{4M_Z^2 s}{ut} - M_Z^4\left(\frac{1}{t^2} + \frac{1}{u^2}\right)\right].$$

(3.5)

Hence the total cross section

$$\sigma_T^Z = \frac{1}{2!} \int_{t_{min}}^{t_{max}} \frac{d\sigma^Z}{dt}\, dt\,,$$

$$t_{max,min} = M_Z^2 - \tfrac{1}{2} s(1 \mp \beta_Z) = -\tfrac{1}{4} s(1\mp\beta_Z)^2\,, \qquad (3.6)$$

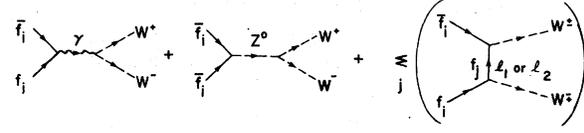$$\beta_Z \equiv \left(1 - \frac{4M_Z^2}{s}\right)^{1/2}$$

becomes

$$\sigma_T^Z = \frac{4\pi\alpha^2}{s} \frac{g_V^{i4}+g_A^{i4}+6g_V^{i2}g_A^{i2}}{e^4}$$
$$\times \left[\frac{1+4M_Z^4/s^2}{1-2M_Z^2/s} \ln\left(\frac{1+\beta_Z}{1-\beta_Z}\right) - \beta_Z\right]. \qquad (3.7)$$

This finishes the preparation for reaction (3.1). The formulas (3.5) and (3.7) can be checked against $ee \to \gamma\gamma$ results if the appropriate limits are taken.

All of the couplings in Eqs. (2.1) and (2.7) come into play in the lowest-order amplitude for reaction (3.2), displayed in Fig. 4. The tensor matrix defined in Fig. 2 reads

$$T_{\mu\nu}^W = i\left(Q_i \frac{e^2}{s} + e_Z \frac{g_V^i+g_A^i\gamma_5}{s-M_Z^2}\right)\left[g_{\mu\nu}(\not{p}_1 - \not{p}_2) + \gamma_\mu(2p_2+p_1)_\nu - \gamma_\nu(2p_1+p_2)_\mu\right]$$

$$-2i(1+\gamma_5)\sum_j G_{V-A}^{ij}{}^2\left[\theta(-Q_i)\frac{\gamma_\mu\not{l}_1\gamma_\nu}{t} + \theta(Q_i)\frac{\gamma_\nu\not{l}_2\gamma_\mu}{u}\right], \qquad (3.8)$$

where the amplitude for fermion f_j exchange requires $W^+ \to W^-$ crossing if $Q_i > 0$.

A long calculation of the unpolarized differential cross section most naturally separates into the squares and interference of the combined s-channel exchange amplitude and the combined t,u exchange amplitude:

$$\frac{d\sigma^W}{dt} = \frac{2\pi\alpha^2}{s^2}\left\{\left[\left(Q_i + \frac{e_Zg_V^i}{e^2} \frac{s}{s-M_Z^2}\right)^2 + \left(\frac{e_Zg_A^i}{e^2} \frac{s}{s-M_Z^2}\right)^2\right]A(s,t,u)\right.$$

$$+4\left[Q_i + \frac{e_Z(g_V^i+g_A^i)}{e^2} \frac{s}{s-M_Z^2}\right]\sum_j (G_{V-A}^{ij}/e)^2[\theta(-Q_i)I(s,t,u) - \theta(Q_i)I(s,u,t)]$$

$$+8\left[\sum_j (G_{V-A}^{ij}/e)^2\right]^2\left.[\theta(-Q_i)E(s,t,u) + \theta(Q_i)E(s,u,t)]\right\}, \qquad (3.9)$$

where

$$A(s,t,u) = \left(\frac{ut}{M_W^4} - 1\right)\left(\frac{1}{4} - \frac{M_W^2}{s} + 3\frac{M_W^4}{s^2}\right) + \frac{s}{M_W^2} - 4\,,$$

$$I(s,t,u) = \left(\frac{ut}{M_W^4} - 1\right)\left(\frac{1}{4} - \frac{1}{2}\frac{M_W^2}{s} - \frac{M_W^4}{st}\right) + \frac{s}{M_W^2} - 2 + 2\frac{M_W^2}{t}\,,$$

$$E(s,t,u) = \left(\frac{ut}{M_W^4} - 1\right)\left(\frac{1}{4} + \frac{M_W^4}{t^2}\right) + \frac{s}{M_W^2}\,. \qquad (3.10)$$

The total cross section,

$$\sigma_T^W = \int_{t_{min}}^{t_{max}} \frac{d\sigma^W}{dt}\, dt\,,$$

(3.11)

$$t_{max,min} = M_W^2 - \tfrac{1}{2}s(1\mp\beta_W) = -\tfrac{1}{4}s(1\mp\beta_W)^2\,, \qquad \beta_W \equiv (1-4M_W^2/s)^{1/2}\,,$$

is then found by inserting

$$\int A(s,t,u)dt = \frac{S^3\beta_W^3}{M_W^4}\left(\frac{1}{24}+\frac{5}{6}\frac{M_W^2}{s}+\frac{1}{2}\frac{M_W^4}{s^2}\right),$$

$$\int I(s,t,u)dt = \int I(s,u,t)dt = \frac{S^3\beta_W}{M_W^4}\left(\frac{1}{24}+\frac{3}{4}\frac{M_W^2}{s}-\frac{7}{6}\frac{M_W^4}{s^2}-\frac{M_W^6}{s^3}\right)-4M_W^2\left(1+\frac{1}{2}\frac{M_W^2}{s}\right)\ln\left(\frac{1+\beta_W}{1-\beta_W}\right), \quad (3.12)$$

$$\int E(s,t,u)dt = \int E(s,u,t)dt = \frac{S^3\beta_W}{M_W^4}\left(\frac{1}{24}+\frac{5}{6}\frac{M_W^2}{s}-2\frac{M_W^4}{s^2}\right)+2s\left(1-2\frac{M_W^2}{s}\right)\ln\left(\frac{1+\beta_W}{1-\beta_W}\right).$$

This completes the groundwork for reaction (3.2).

IV. ELECTRON-POSITRON EXPERIMENTS

We now discuss electron-positron colliding beams and the numerical results for the pair-production cross sections. Specifically, the reactions (3.1) and (3.2) are

$$e^+ + e^- \rightarrow Z^0 + Z^0 \qquad (4.1)$$

and

$$e^+ + e^- \rightarrow W^+ + W^-. \qquad (4.2)$$

The numbers come from the formulas in Sec. III adapted to $f_i = e^-$.

The total cross section for reaction (4.1) is calculated from Eq. (3.7) using the couplings determined by Eqs. (2.4) and (2.5). The results for the
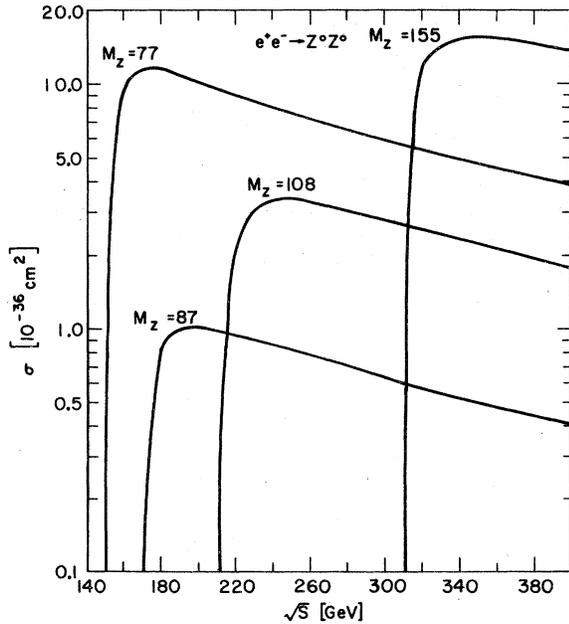
range (2.16) are plotted in Fig. 5 and the nonmonotonic behavior as a function of M_Z is due to the couplings' dependence on x. The culprit is the factor

$$g_V^{e4}+g_A^{e4}+6g_V^{e2}g_A^{e2}$$
$$=\left(\frac{e_N}{2}\right)^4[1+(4x-1)^4+6(4x-1)^2]. \quad (4.3)$$

The square bracket has a minimum at $x=\frac{1}{4}$ or $M_Z \approx 88$ GeV/c^2. We can relax the constraint between M_Z and x by keeping (2.6) and denying (2.12). The idea is to use

$$\frac{e_N}{2e}=\frac{M_Z}{2^{3/4}}\left(\frac{G_F}{4\pi\alpha}\right)^{1/2}\simeq 6.2\times 10^{-3}\frac{M_Z}{M_P} \quad (4.4)$$

in (4.3). This will give the same low-energy limit since M_Z cancels out, and total cross sections are shown in Fig. 6.
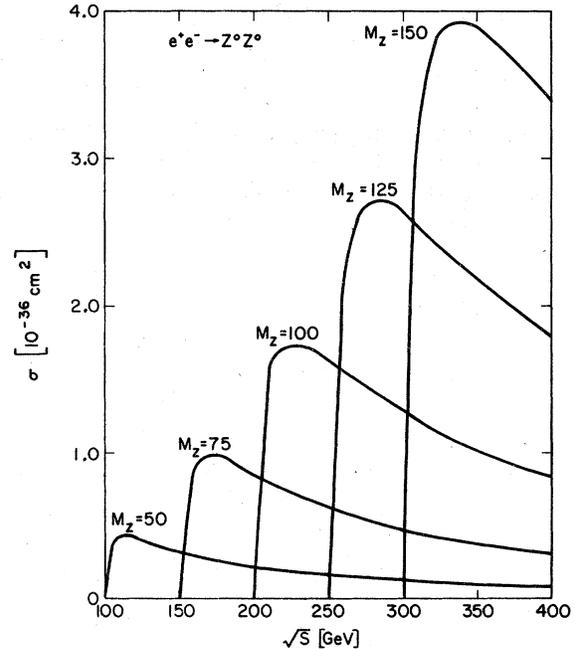

FIG. 5. Total cross sections, in units of 10^{-36}cm^2, for $e^+e^-\rightarrow Z^0Z^0$ in the Weinberg–Salam gauge theory. The mass range is that of Eq. (2.16) where x follows range (2.15) (x must be the independent variable since both θ_W and $\pi/2 - \theta_W$ give the same M_Z).

FIG. 6. Total cross sections, in units of 10^{-36} cm^2, for $e^+e^-\rightarrow Z^0Z^0$ in a V,A theory where the couplings have been chosen to be consistent with Eqs. (2.4)–(2.6) but with M_Z independent of x. Note that here $\sigma_T^Z/S = f(S/M_Z^2)$.
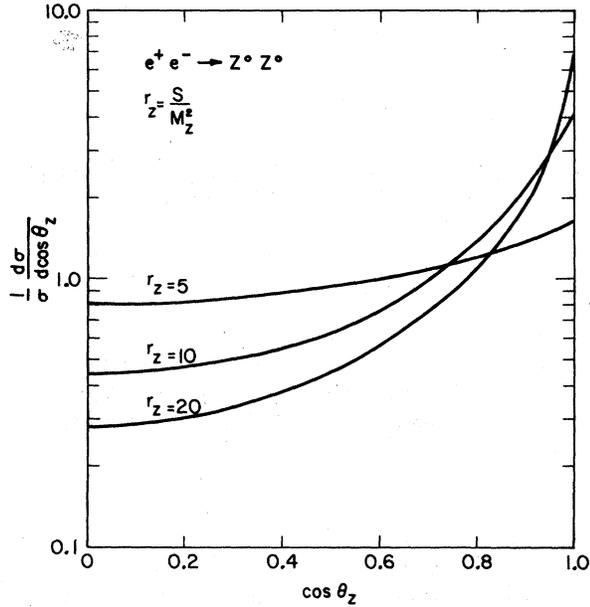
FIG. 7. Differential cross section for $e^+e^- \to Z^0Z^0$; Here $r_Z = s/M_Z^2$. The $\cos\theta_Z < 0$ range is not shown in view of the Bose symmetry.

To find out where these events lie in angle, we plot $1/\sigma_T^Z d\sigma^Z/d\cos\theta_Z$ in Fig. 7. [Note that $dt = \frac{1}{2}s\beta_Z d\cos\theta_Z$ in Eq. (3.5).] It should be mentioned that this ratio scales,

$$\frac{1}{\sigma_T^Z}\frac{d\sigma^Z}{d\cos\theta_Z} = f(r_Z, \cos\theta_Z),$$

$$r_Z \equiv \frac{s}{M_Z^2}, \tag{4.5}$$

since the couplings cancel out. Therefore the plot can be used for arbitrary M_Z values. Roughly speaking, the curves are peaked inside of $\theta_Z \simeq M_Z^2/s$, a result due to the electron propagator enhancement.

We should also mention that the numbers in Fig. 6 would lie on one universal curve if we had plotted

σ_T^Z/s versus r_Z. This is not true for the Weinberg-Salam theory.

As a contrasting prelude to the interesting aspect of W^+W^- pair production, the (acceptable) high-energy behavior $\sigma_T^Z \propto (1/s)\ln s$ does not depend on coupling-constant interrelationships. The only important cancellation, related to electromagnetic gauge invariance, is between the t and u exchanges for the $P_\mu P_\nu/M_Z^2$ longitudinal part of the polarization factor. This has nothing to do with non-Abelian gauge principles.

But reaction (4.2) is a practical example of where the gauge theories do become important to us. Renormalizability translates into cancellations among the graphs in Fig. 4 so that unitarity bounds are not a problem. The resulting $\sigma_T^W \propto (1/s)\ln s$ behavior *does* depend on coupling constants as is well known. Specifically, one can see that the linear and constant terms (in s) cancel out in σ_T^W [see (3.9)–(3.12)] if

$$Q_i e^2 + e_Z g_V^i - 2\,\text{sgn}(Q_i)\sum_j (G_{V-A}^{ij})^2 = 0 \tag{4.6}$$

and

$$e_Z g_A^i - 2\,\text{sgn}(Q_i)\sum_j (G_{V-A}^{ij})^2 = 0, \tag{4.7}$$

a fact that is more obvious from the amplitude itself. These are true for all i in the standard non-Abelian gauge model, of course, and (4.6) and (4.7) could be written without the signum function since

$$a_i = \frac{1}{2}\,\text{sgn}(Q_i) - 2Q_i x,$$
$$b_i = \frac{1}{2}\,\text{sgn}(Q_i). \tag{4.8}$$

In detail, $i = e$ and $j = \nu$ for the reaction (4.2). Equations (3.9)–(3.12) reduce to formulas which have been checked against previous calculations by Allès *et al.*[10] For completeness, we repeat the answers:

$$\frac{d\sigma^W(ee)}{dt} = \frac{\pi\alpha^2}{4s^2x^2}\left\{A(s,t,u) - 2I(s,t,u) + E(s,t,u)\right.$$

$$\left. + \frac{2(1-2x)}{r_Z - 1}[A(s,t,u) - I(s,t,u)] + \frac{1 - 4x + 8x^2}{(r_Z - 1)^2}A(s,t,u)\right\}$$

and

$$\tag{4.9}$$

$$\sigma_T^W(ee) = \frac{\pi\alpha^2}{2sx^2}\left[W_1(r_W) + \frac{1-2x}{r_Z - 1}W_2(r_W) + \frac{1-4x+8x^2}{(r_Z-1)^2}W_3(r_W)\right],$$

$$W_1 \equiv \left(1 + \frac{2}{r_W} + \frac{2}{r_W^2}\right)\ln\left(\frac{1+\beta_W}{1-\beta_W}\right) - \frac{5}{4}\beta_W, \quad W_2 \equiv \frac{4}{r_W}\left(1 + \frac{1}{2r_W}\right)\ln\left(\frac{1+\beta_W}{1-\beta_W}\right) - \frac{1}{12}\beta_W r_W\left(1 + \frac{20}{r_W} + \frac{12}{r_W^2}\right),$$

$$W_3 \equiv \frac{1}{48}\beta_W^3 r_W^2\left(1 + \frac{20}{r_W} + \frac{12}{r_W^2}\right), \quad r_W \equiv s/M_W^2. \tag{4.10}$$

To compare these to the $Z^0 Z^0$ answers, the total and differential cross sections are shown in Figs. 8 and 9, respectively, for the M_W and r_W values of interest to us. These curves are complementary to the published curves.[10] In contrast to the neutral-boson case, we cannot keep the low-energy limits intact while changing M_W. The high-energy cancellation requires all of the Weinberg-Salam constraints, noting $g^i_{V,A} \propto M_Z$ and $G^{ij}_{V-A} \propto M_W$. The only feasible way to vary M_W is by changing x. Notice that $s > M_Z^2$ for all of the M_W values considered ($\theta_W < 60°$ or $x < \frac{3}{4}$) so the Z^0 resonance region is not breached.

The reader can interpolate the total cross sections for reaction (4.2) to different mass values by the simple approximation for $M_W \geq 50$ (in units of GeV/c^2):

$$\sigma_T^W(ee) \simeq F^W(M_W/50)H^W(s/4M_W^2),$$

$$F^W(z) \equiv 2.2[1 + 4.5(\ln z)^{2 \cdot 2}] \times 10^{-35} \text{ cm}^2,$$

$$H^W(z) \equiv \frac{1}{Z}[\beta(z)\ln z]^{0 \cdot 3}, \tag{4.11}$$

$$\beta(z) \equiv (1 - 1/z)^{1/2}.$$

This gives 20% accuracy and shows rough scaling behavior. For comparison with (4.11), and with the subsequent fits to the proton results, the total cross section for reaction (4.1) can be approxi-
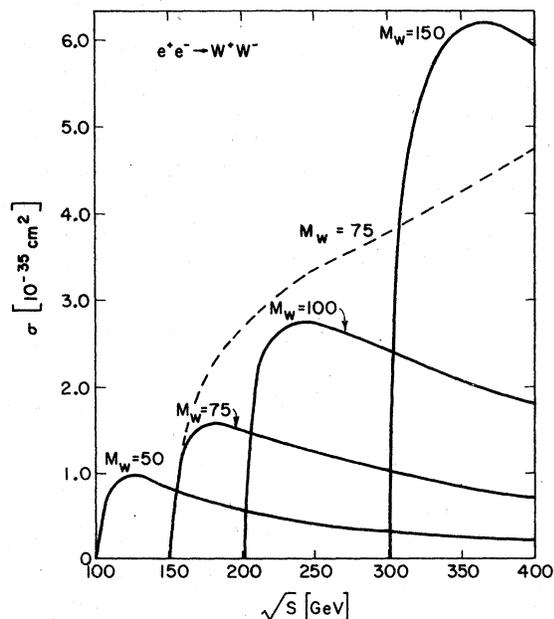
FIG. 9. Differential cross section $e^+e^- \to W^+W^-$. Here θ_{W^-} is the angle between e^- and W^-. For comparison, the r_W values are identical to the r_Z values of Fig. 7. In contrast to Fig. 7, there is no scaling here in r_W.

mated by

$$\sigma_T^Z(ee) \simeq F^Z(x)H^Z(s/4M_Z^2),$$

$$F^Z(x) \equiv 0.37 \, \frac{1 + (4x-1)^4 + 6(4x-1)^2}{x(1-x)} \times 10^{-36} \text{ cm}^2$$

$$H^Z(z) \equiv \frac{1}{z}[\beta(z)\ln z]^{0 \cdot 19} \tag{4.12}$$

in the Weinberg-Salam model, although the "exact" answer is not much more complicated.

Figure 8 also includes a representative curve which corresponds to a calculation in which there are no gauge cancellations. It is the result of dropping the Z^0 graph altogether and shows striking growth in energy.

V. PROTON-PROTON AND PROTON-ANTIPROTON EXPERIMENTS

The other reactions of interest to us in pair production involve colliding proton beams

$$p + p \to Z^0 + Z^0 + X, \tag{5.1}$$

$$p + p \to W^+ + W^- + X, \tag{5.2}$$

and colliding proton-antiproton beams

$$p + \bar{p} \to Z^0 + Z^0 + X, \tag{5.3}$$

$$p + \bar{p} \to W^+ + W^- + X. \tag{5.4}$$

We use the quark-parton model in these high-energy inclusive reactions where X implies a sum over all unobserved additional debris. The collisions are viewed as collisions of quarks (spec-

FIG. 8. Total cross sections, in units of 10^{-35} cm^2, for $e^+e^- \to W^+W^-$ in the Weinberg-Salam gauge theory. The mass range is discussed in Sec. II; its units are GeV/c^2. The dashed line is an example of a calculation without the high-energy cancellation.

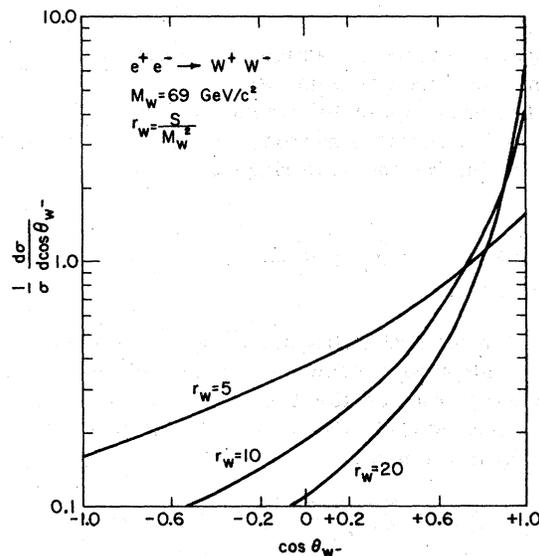ifically, quarks and antiquarks in the dominant amplitude discussed below).

The prescription for calculating cross sections involving an initial hadron with four-momentum p is the incoherent scattering formula[11]

$$d\sigma(p,\ldots) = \sum_i \int d\sigma_i(xp,\ldots)P_i(x)\,dx\,. \qquad (5.5)$$

$P_i(x)$ is the probability of finding the ith parton in that hadron with momentum xp and $d\sigma_i$ is the elementary cross section for the parton as an initial collider. More to the point, two colliding hadrons are analyzed using

$$d\sigma(p_1,p_2) = \sum_{i,j} \int\int d\sigma_{ij}(xp_1, yp_2,\ldots)$$

$$\times P_i(x)P_j(y)\,dx\,dy\,. \qquad (5.6)$$

The success (to the accuracy we desire) of the Drell-Yan mechanism for muon pairs suggests that we consider the dominant contributions corresponding to Fig. 10. They give

$$\sigma(AB \to C\overline{C}X) = \sum_i \int\int_{\text{threshold}}^1 dx_A\,dx_B P_i^A(x_A)$$

$$\times P_i^B(x_B)\sigma_T(q_i\bar{q}_i \to C\overline{C})\,. \qquad (5.7)$$

If we change variables[11] to x and τ,

$$x = x_A - x_B\,,$$
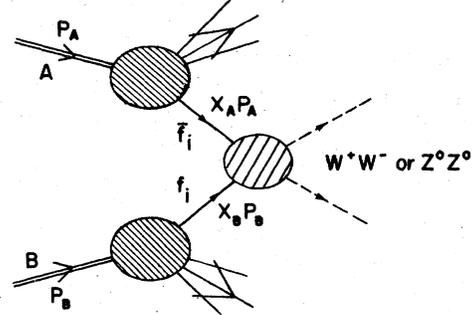
$$\tau = x_A x_B = Q^2/S\,,$$

FIG. 10. The Drell-Yan mechanism for weak-boson pair production. f_i is either a quark or an antiquark. A (B) is a proton (proton or antiproton).

with

$$Q^2 \equiv (p_C + p_{\overline{C}})^2 = (x_A p_A + x_B p_B)^2$$

$$= 2x_A x_B p_A \cdot p_B\,,$$

$$S \equiv (p_A + p_B)^2 = 2p_A \cdot p_B\,, \qquad (5.8)$$

we have the double-differential cross section

$$\frac{d\sigma(AB \to C\overline{C}X)}{d\tau\,dx} = \frac{1}{(x^2+4\tau)^{1/2}}\frac{1}{3}$$

$$\times \sum_{i=u,d,s,c} [P_i^A(x_A)P_i^B(x_B)$$

$$+ P_i^A(x_A)P_i^B(x_B)]\sigma_T(q_i\bar{q}_i \to C\overline{C})\,. \qquad (5.9)$$

The quark-antiquark total cross section σ_T at Q^2 c.m. energy-squared has been prepared in Sec. III for $C\overline{C} = W^+W^-$ or Z^0Z^0. The distributions P_i are summed over color; the factor $\frac{1}{3}$ is needed since $q_i\bar{q}_i$ must have zero color.

In terms of an integration over the original x_A,

$$\frac{d\sigma(AB \to C\overline{C}X)}{d\tau} = \frac{1}{3}\sum_{i=u,d,s,c}\int_\tau^1 \frac{dx_A}{x_A}\,[P_i^A(x_A)P_i^B(\tau/x_A) + P_i^A(x_A)P_i^B(\tau/x_A)]\sigma_T(q_i\bar{q}_i \to C\overline{C})\,, \qquad (5.10)$$

and finally

$$\sigma_T(AB \to C\overline{C}X) = \int_{4M^2/S}^1 \frac{d\sigma}{d\tau}\,d\tau\,, \qquad (5.11)$$

$$M = M_Z, M_W\,.$$

These integrals are evaluated numerically.

The probability functions are determined from fits to the deep-inelastic data on $ep \to eX$ and $pp \to \mu^+\mu^-X$ using the quark-parton interpretation.

We use the parametrizations[12] $P_i(x)$ for the *proton*,

$$P_u = \frac{1.74}{\sqrt{x}}(1-x)^3(1+2.3x)+S(x)\,,$$

$$P_d = \frac{1.11}{\sqrt{x}}(1-x)^{3.1}+S(x)\,, \qquad (5.12)$$

$$P_s = P_{\bar{s}} = P_{\bar{u}} = P_{\bar{d}} = S(x)\,,$$

$$P_c = P_{\bar{c}} \simeq 0\,,$$

in terms of the sea distribution

$$S(x) = \frac{0.51}{x}(1-x)^{10}\,. \qquad (5.13)$$
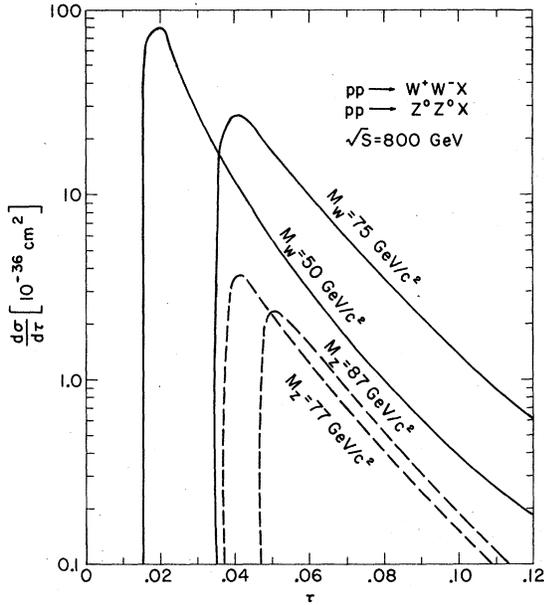
We have thus neglected the charm content of the

FIG. 11. Invariant-mass distributions in units of 10^{-36} cm^2, for W and Z^0 pair production in proton-proton collisions.

sea. For *antiprotons*, read $u \rightarrow \bar{u}$ and $d \rightarrow \bar{d}$.

In Fig. 11 we plot the differential cross section $d\sigma/d\tau$ for the proton-proton reactions (5.1) and (5.2). The same function for the antiproton-proton reactions (5.3) and (5.4) is plotted in Fig. 12. We have chosen an ISABELLE energy ($S = 6.4 \times 10^5$ GeV^2) and boson masses corresponding to the first half of the range discussed in Sec. II. The general
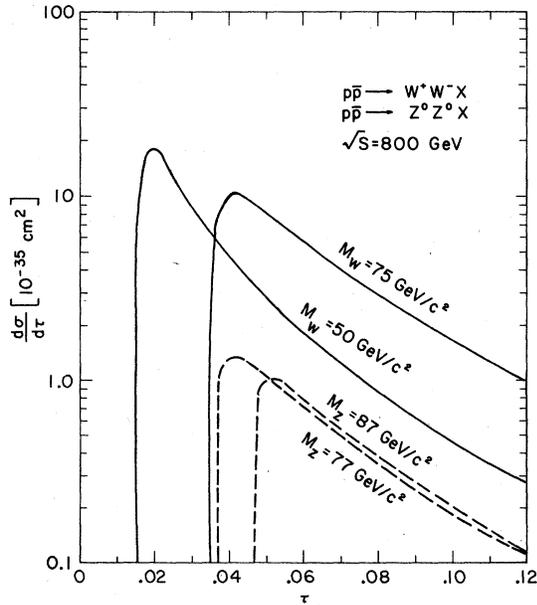

FIG. 12. Invariant-mass distribution, in units of 10^{-35} cm^2, for W and Z^0 pair production in proton-antiproton collisions.
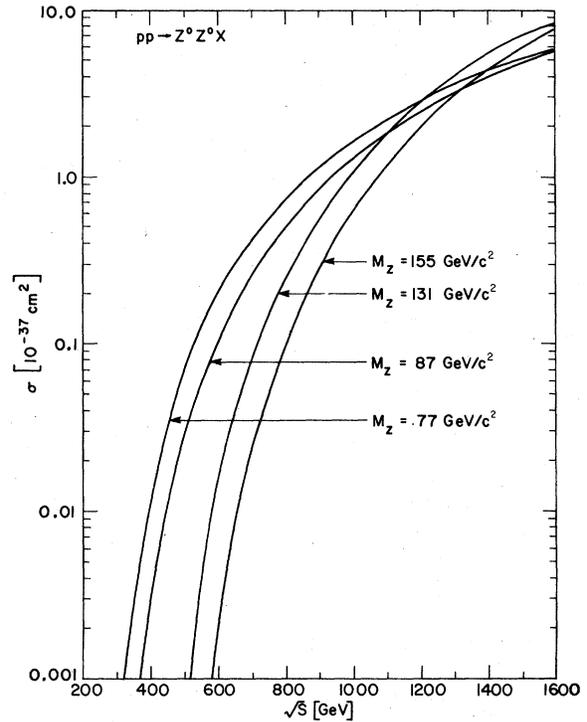

FIG. 13. Total cross sections, in units of 10^{-37}cm^2, for $pp \rightarrow Z^0 Z^0 X$.

shapes are independent of such parameters; they are just what you expect from the basic $q\bar{q}$ cross section and the x_A "phase space." (The probability functions peak in the same direction.)
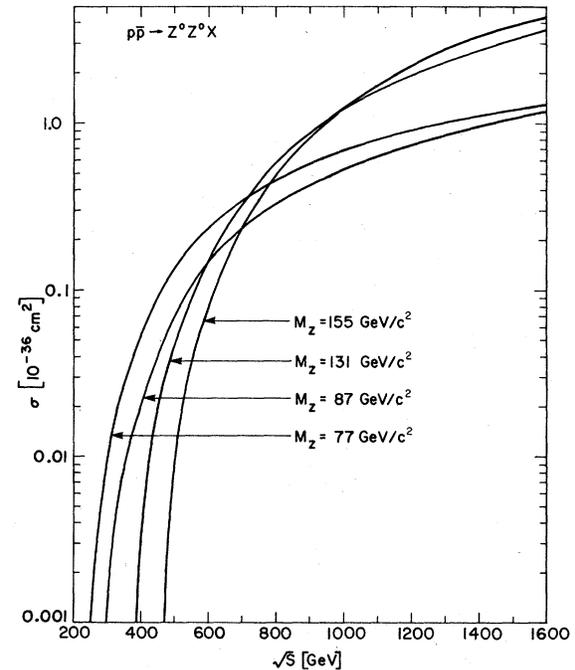

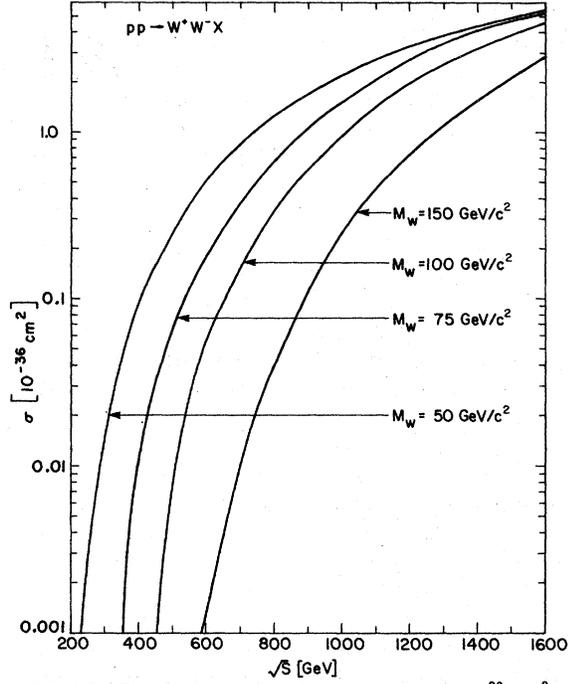FIG. 14. Total cross sections, in units of 10^{-36} cm^2, for $p\bar{p} \rightarrow Z^0 Z^0 X$.

FIG. 15. Total cross sections, in units of 10^{-36} cm^2, for $pp \rightarrow W^+ W^- X$.

While we are on the subject of $q\bar{q}$ cross sections, the important cancellations mentioned in Sec. IV for $e^+ e^-$ occur here as well (for large Q^2). The additional feature here in such cancellations is the role of the two contributions to the quark-exchange
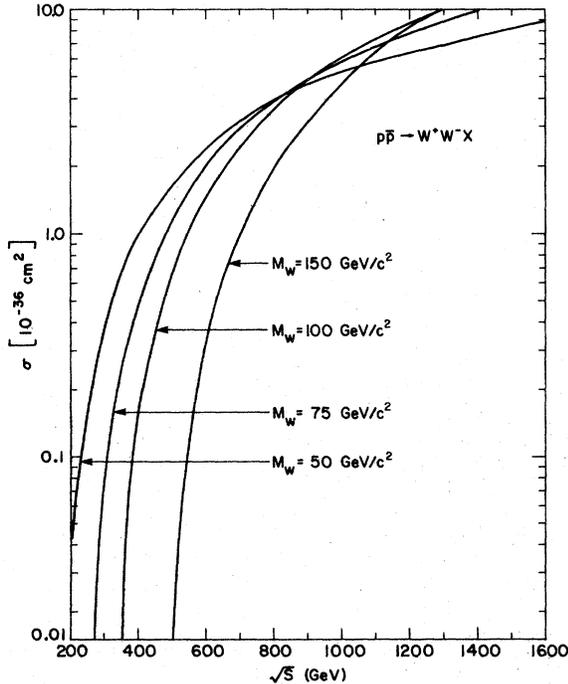

FIG. 16. Total cross sections, in units of 10^{-36} cm^2, for $p\bar{p} \rightarrow W^+ W^- X$.

diagrams. Notice

$$\sum_j \left(G^{ij}_{V-A} \right)^2 = \frac{M_W^2 G_F}{\sqrt{2}} = e_W^2 \qquad (5.14)$$

for all i. When $i = d, s$, for example, then $j = u, c$ and we get the overall factor $\cos^2 \theta_C + \sin^2 \theta_C = 1$. The Cabibbo angle cancels out in the "neutrino" diagram by itself, as it must since there is no other θ_C dependence. This is nothing other than the need for charm if quark gauge theories are to be renormalizable.[13]

The total cross sections are presented in Figs. 13–16. The full boson mass range discussed in Sec. II is covered. We see that the rates, for the same flux, are in favor of the $p\bar{p}$ beam just as in the case of muon pair production. Antiprotons have valence antiquarks. For the same reason, the pp case is very sensitive to the sea distribution parametrization.

We have made the same sacrifice of varying θ_W in order to vary M_W and M_Z. This is particularly of concern since the quark neutral-current couplings are constrained from neutrino-nucleon scattering.[14] One really needs a different theory for masses other than (2.11).

The minimum in the bracket of Eq. (4.3) at $x = \frac{1}{4}$ has counterparts here. For example,

$$g_V^{u4} + g_A^{u4} + 6 g_V^{u2} g_A^{u2}$$

$$= \left(\frac{e_N}{2} \right)^4 [1 + (\tfrac{8}{3} x - 1)^4 + 6(\tfrac{8}{3} x - 1)^2] , \qquad (5.15)$$

with a minimal bracket value at $x = \frac{3}{8}$ or $M_Z \approx 78$ GeV/c^2. The vector coupling vanishes at the same place for the charm quark and at $x = \frac{3}{4}$ or $M_Z \approx 88$ GeV/c^2 for the down and strange quarks. Such an effect gets smeared out over these mass values when we sum over the quarks but it is seen in Figs. 13 and 14. In contrast, we see the expected "crossover" pattern in the W-pair production cross sections of Fig. 16.

It is possible to parametrize the curves in these last four figures in terms of simple fits. The formulas analogous to those in Eq. (4.11) are

$$\sigma_T^Z(pp) \simeq 3.3 \times 10^{-41} K(x, 2.5)$$

$$\times L(s/4M_Z^2; 11.7, 5) \text{ cm}^2 ,$$

$$\sigma_T^Z(p\bar{p}) \simeq 2.7 \times 10^{-39} K(x, 2.6)$$

$$\times L(s/4M_Z^2; 5.4, 2.5) \text{ cm}^2 ,$$

$$\sigma_T^W(pp) \simeq 2.8 \times 10^{-39} J(M_W/50; 5.3, 2) \qquad (5.16)$$

$$\times L(s/4M_W^2; 15.5, 4.45) \text{ cm}^2 ,$$

and

$$\sigma_T^W(p\bar{p}) \simeq 1.3 \times 10^{-37} J(M_W/50; 8.8, 2.4)$$

$$\times L(s/4M_W^2; 9.9, 2.5) \text{ cm}^2 ,$$

where

$$K(x, a) \equiv [1 + (ax - 1)^4 + 6(ax - 1)^2]/x(1 - x),$$

$$L(z; \alpha, \beta) \equiv (1 - 1/z)^\alpha (\ln z)^\beta, \qquad (5.17)$$

$$J(z; a, b) \equiv 1 + a(\ln z)^b.$$

On the average, these formulas reproduce our curves in Figs. 13 through 16 with an accuracy of about 25%.

VI. DISCUSSION

Let us first review the electron-colliding-beam expectations for weak-boson physics in order to see just where our calculations fit into the picture. Most attention[5] for the generation of machines beyond PEP and PETRA has been paid to what can be learned by tuning in the Z^0 resonance or at least through its interference effects in $ee \rightarrow \mu\mu$. Beyond that, the energies contemplated *are* large enough to consider W^+W^- pair production. This is important because single-W production may be too rare. (There is the $ee \rightarrow WX$ possibility,[15] but with signature and background problems which may sap the strength of electron-positron collisions: their cleanliness.) Probably more important, since the W is likely to be found elsewhere first, is that the $ee \rightarrow WW$ reaction shows us how the renormalization program is working and exposes the electromagnetic coupling of the W and the trilinear boson coupling. This motivation forms the basis for previous interest[5,10] in such a reaction and our results for $ee \rightarrow WW$ are not new. On our way to proton experiments, we simply digressed in order to check these earlier formulas and we have presented a few additional curves and a parametrization.

The Z^0 will presumably be seen first as a resonance. (Its width is much larger than those associated with the ψ search at SPEAR and the Υ search[16] at DORIS). But if the energies are large enough to produce W pairs, then we point out in this paper that Z^0Z^0 pairs can be of interest. The calculation is perhaps too simple; gauge theories are not needed to control the high-energy behavior and only the mass and the neutral-current couplings come into play.

It should be noted at this point that there is interest in additional neutral bosons in those gauge models which explain the absence of parity violations in atomic physics.[17] These may be as light as 30 GeV/c^2 and add to the importance of exploring Z^0 production possibilities. It is not hard to correct our numbers to different models; the important $g \propto M_Z$ relation is already included.

If the weak bosons do exist, the consensus is that they will be found in proton-proton or proton-

antiproton colliding-beam experiments. Since it is quite possible that the threshold for pair production may also be reached with the same machine, we have been drawn toward that possibility in this work. We have seen that the total cross sections for pairs is down by roughly three orders of magnitude. The cross sections for $pp \rightarrow WX$ are typically 10^{-34}–10^{-33} cm^2 for $S/M^2 \approx 10$. Thus the original hope[18] that pairs may be more easily identified is probably too optimistic (the gauge cancellation among the three Feynman diagrams takes effect already rather close to threshold). The pair search will have to wait for "state-of-the-art" development as the new machines are put into operation.

Even if the pair production of weak bosons cannot be taken seriously as a primary search mode, we feel it has an important place in the future. The point is that the gauge cancellations—the renormalizability question—can be "seen" in the W^+W^- production (recall the $d\sigma/d\tau$ plot). This would be the first example of weak-electromagnetic cross sections brought under control at high energies; electron colliding beams of sufficient energy will not be built until years after the proton machines go into operation. The remarks made before about the electromagnetic interaction of the W's and the trilinear coupling ZWW as well as the cancellation in the $ee \rightarrow WW$ context thus carry yet more weight here. Besides, we also have the Glashow-Iliopoulos-Maiani mechanism[13] at work. (This energy-time advantage for proton machines may also be true for other contexts: The Z^0-γ interference in muon pairs and all the information it gives us about couplings may be manifested first in proton collisions.[19]) We remind the readers that without the gauge cancellations, weak interactions will prove to be strong at such energies; higher-order contributions will necessarily force a leveling off of $d\sigma/d\tau$ but probably for τ values rather larger than seen in Fig. 11. The modified theory operates early on. By contrast, a non-gauge theory result would look like the curve in Fig. 8.

If we believe in the importance of pair production, can we also believe in our calculation? The questions are whether the Drell-Yan model is applicable at higher energies and whether we have used it correctly with respect to known lower-energy results. The covering quantum chromodynamics (QCD) theory of quarks and gluons may require some additional diagrams such as quark-quark and quark-gluon scattering and accordingly may tell us that we have not put in the correct sea-quark distributions—distributions which are checked phenomenologically *assuming* Drell-Yan dominance.[20] If we interpret the QCD assessment

correctly, however, this is not of great concern since we are satisfied with order-of-magnitude estimates.

Beyond the τ dependence, the angular distribution for the bosons in the proton-antiproton collision follows essentially from the e^+e^- $\cos\theta$ plot in Fig. 9. After the cancellations we have spoken about so often, the dominance of the d exchange amplitude in $u\bar{u}$ annihilation leads to peaking at small angles. The W^+ (W^-) is preferentially emitted along the proton (antiproton) initial direction. The $d\bar{d}$ annihilation reverses this preference but is less important. The sea is negligible here. The identical Z^0's are found in both forward and backward cones, of course. The characteristic angle for peaking is $\theta \approx M^2/\langle Q^2 \rangle$ where $\langle Q^2 \rangle = S\langle\tau\rangle$. Figures 11 and 12 give one an idea about $\langle\tau\rangle$. The identical proton-proton collisions lead to peaking in both directions for W^+W^- as well as Z^0Z^0. The larger $\langle x \rangle$ value for the valence quark (as compared with the sea antiquark) squeezes the W^+ closer to the beam line (forward or backward) in contrast to the W^-. The neglected proton transverse momentum is reported to be unimportant in single-W production[7] and so we assume that to be the case for pair production as well.

The branching ratios of 5% for $Z^0 \rightarrow \mu^+\mu^-$ and 12% for $W \rightarrow \mu\nu$ or $W \rightarrow e\nu$ are quoted most often[7] as the relevant signature weights in single W searches. The large hadronic branching ratios may work against single W or Z^0 searches if the hadronic jet is buried under other high-p_T processes of quite different origins. Pair production, however, would lead to double jets which may be more distinctive events. In addition, μ-e, μ-jet, and other combinations may also be viable signatures. Nat-

urally, the $\mu^+\mu^-$ invariant distribution nails down the Z^0.

We have not considered the reaction $pp \rightarrow WZ + X$, but the expectations are the same. There is no photon intermediary but both t and u exchange graphs arise and the small-angle peaking persists. Also, anomalous electromagnetic moments for the Z^0 as well as for the W (changing μ_W and Q_W) ruin renormalizability and would show up in the high-energy behavior of the cross sections. We have neglected them.

It is hoped that the simple formulas given as fits to our cross-section curves will be useful for other energy-mass regimes. These can often be quite accurate in other W production reactions. We are at present working on an updating and review of the various beam possibilities where such fits will be presented.

Note added. We have now calculated WZ pair production, a calculation which involves the changes described above. This is of interest in very-high-energy cosmic neutrino physics as well as for completing the pp and $\bar{p}p$ picture. A forthcoming report contains details. We should mention that the exciting polarization SLAC experiment [C. Y. Prescott *et al.*, Phys. Lett. **77B**, 347 (1978)] implies $x \simeq 0.20$ or $M_W \simeq 84$ GeV/c^2, $M_Z \simeq 94$ GeV/c^2.

*Present address: Department of Physics, Oklahoma State University, Stillwater, Oklahoma 74074.

[1]S. Weinberg, Phys. Rev. Lett. **19**, 1264 (1967); **27**, 1688 (1971); A. Salam, in *Elementary Particle Theory: Relativistic Groups and Analyticity (Nobel Symposium No. 8)*, edited by N. Svartholm (Almqvist and Wiksell, Stockholm, 1968), p. 367.

[2]B. C. Barish, Phys. Rep. **39C**, 279 (1978). The absence of direct production with neutrino beams indicates $M_W \gtrsim 8$ GeV/c^2. The absence of a propagator effect implies $M_W \gtrsim 30$ GeV/c^2.

[3]H. Harari, Phys. Rep. **42C**, 235 (1978). This includes the discussion of heavier quarks and parity violation.

[4]BNL Report No. 50648, 1977 (unpublished).

[5]Representative are CERN Reports Nos. CERN 76-18 (unpublished) and CERN 76-12 (unpublished).

[6]See the first report cited in Ref. 5.

[7]See the calculations and review by C. Quigg, Rev. Mod. Phys. **49**, 297 (1977). A recent, thorough study has also been done by R. F. Peierls, T. F. Trueman, and L. L. Wang, Phys. Rev. D **16**, 1397 (1977). Asymptotic freedom is considered by J. Kogut and J. Shigemitsu, Nucl.

Phys. **B129**, 461 (1977).

[8]For a general review, see E. S. Abers and B. W. Lee, Phys. Rep. **9C**, 1 (1973).

[9]We follow the conventions and notation of J. D. Bjorken and S. D. Drell, *Relativistic Quantum Fields* (McGraw-Hill, New York, 1965). The weak-boson field W creates W^+ and destroys W^- single-particle states. For us, $e = + (4\pi\alpha)^{1/2} \simeq 0.30$, $G_F \simeq 10^{-5}/M_P^2$. M_i refers to the mass of particle i and $\not{a} \equiv \gamma_\mu a^\mu$. Electron, quark and proton masses are neglected throughout.

[10]W. Allès, Ch. Boyer, and A. J. Buras, Nucl. Phys. **B119**, 125 (1977); O. P. Sushkov, V. V. Flambaum, and I. B. Khriplovich, Yad. Fiz. **20**, 1016 (1974) [Sov. J. Nucl. Phys. **20**, 537 (1975)]; G. Komen, Nucl. Phys. **B84**, 323 (1975); F. Blezacker and H. T. Nieh, *ibid.* **B124**, 511 (1977). For pre-gauge-theory discussion, see N. Cabibbo and R. Gatto, Phys. Rev. **124**, 1577 (1961); Y. -S. Tsai and A. C. Hearn, *ibid.* **140**, 721 (1965).

[11]We use the notation of Quigg, Ref. 7. Beware of the double role that x plays in our equations.

[12]J. Okada, S. Pakvasa, and S. F. Tuan, Lett. Nuovo Cimento **16**, 555 (1976); D. M. Kaplan *et al.*, Phys.

Rev. Lett. 40, 435 (1978).

[13]S. L. Glashow, J. Iliopoulos, and L. Maiani, Phys. Rev. D 2, 1285 (1970).

[14]L. F. Abbott and R. Michael Barnett, Phys. Rev. Lett. 40, 1303 (1978).

[15]F. M. Renard and M. Talon, Phys. Lett. 67B, 59 (1977).

[16]C. W. Darden et al., Phys. Lett. 76B, 246 (1978).

[17]See, for example, R. N. Mohapatra and D. P. Sidhu, Phys. Rev. D 18, 856 (1978); V. Barger and R. J. N. Phillips, ibid. 18, 775 (1978) and references therein.

[18]A preliminary estimate of W pair production has been made by one of us: K. O. Mikaelian, ISABELLE Summer Study Proceedings (Brookhaven), 1975 (unpublished) Vol. II, p. 340.

[19]R. W. Brown, K. O. Mikaelian, and M. K. Gaillard, Nucl. Phys. B75, 112 (1974); Michigan, Northeastern, and Washington collaboration, Fermilab Proposal No. 583 (unpublished).

[20]H. Georgi. Phys. Rev. D 17, 3010 (1978).